Durham University

Durham Research Online

Deposited in DRO:

15 February 2010

Version of attached file:

Published Version

Peer-review status of attached file:

Peer-reviewed

Citation for published item:

Dominy, R. and Lunt, P. and Bickerdyke, A. and Dominy, J (2007) 'Self-starting capability of a Darrieus turbine.', Proceedings of the I MECH E part A : journal of power and energy., 221 (1). pp. 111-120.

Further information on publisher's website:

http://dx.doi.org/10.1243/09576509JPE340

Publisher's copyright statement:

Dominy, R. and Lunt, P. and Bickerdyke, A. and Dominy, J., 2007. The definitive, peer reviewed and edited version of this article is published in Proceedings of the I MECH E part A : journal of power and energy, 221, 1, pp. 111-120, 10.1243/09576509JPE340

Additional information:

Use policy

The full-text may be used and/or reproduced, and given to third parties in any format or medium, without prior permission or charge, for personal research or study, educational, or not-for-profit purposes provided that:

- a full bibliographic reference is made to the original source
- a link is made to the metadata record in DRO
- the full-text is not changed in any way

The full-text must not be sold in any format or medium without the formal permission of the copyright holders.

Please consult the full DRO policy for further details.

Durham University Library, Stockton Road, Durham DH1 3LY, United Kingdom
Tel : +44 (0)191 334 3042 — Fax : +44 (0)191 334 2971
http://dro.dur.ac.uk

Durham University

Durham Research Online

Deposited in DRO:
15 February 2010

Peer-review status:
Peer-reviewed

Publication status:
Published version

Citation for published item:
Dominy, R. and Lunt, P. and Bickerdyke, A. and Dominy, J (2007) 'Self-starting capability of a Darrieus turbine.', *Proceedings of the I MECH E part A : journal of power and energy*., 221 (1). pp. 111-120.

Further information on publisher's website:
http://dx.doi.org/10.1243/09576509JPE340

Publisher's copyright statement:
© Dominy, R. and Lunt, P. and Bickerdyke, A. and Dominy, J., 2007. The definitive, peer reviewed and edited version of this article is published in *Proceedings of the I MECH E part A : journal of power and energy*, 221, 1, pp. 111-120, 10.1243/09576509JPE340

Use policy

The full-text may be used and/or reproduced, and given to third parties in any format or medium, without prior permission or charge, for personal research or study, educational, or not-for-profit purposes provided that :

- a full bibliographic reference is made to the original source
- a link is made to the metadata record in DRO
- the full-text is not changed in any way

The full-text must not be sold in any format or medium without the formal permission of the copyright holders.

Please consult the full DRO policy for further details.

Durham University Library, Stockton Road, Durham DH1 3LY, United Kingdom
Tel : +44 (0)191 334 2975 | Fax : +44 (0)191 334 2971
http://dro.dur.ac.uk

Self-starting capability of a Darrieus turbine

R Dominy[1]*, **P Lunt**[1], **A Bickerdyke**[1], and **J Dominy**[2]
[1]School of Engineering, University of Durham, Durham, UK
[2]Carbon Concepts Limited, Unit A2, Lower Mantle Close, Derbyshire, UK

The manuscript was received on 10 July 2006 and was accepted after revision for publication on 14 September 2006.

DOI: 10.1243/09576509JPE340

Abstract: Darrieus-type vertical axis wind turbines have a number of potential advantages for small-scale and domestic applications. For such applications, the issues of cost and reliability are paramount and hence simplicity of design of the structure, the generator, and any control system is vital. A particular concern relating to Darrieus turbines is their potential to self-start. If, as has been suggested by several authors, they require external assistance to start then much of their advantage is lost. The purpose of the study described here is, therefore, to investigate their starting performance through the development and validation of computational simulation and to determine the parameters that govern the capability to self-start. A case study is presented based upon the use of the widely used and well documented, symmetrical NACA 0012 turbine blade profile. It is shown that a lightly loaded, three-bladed rotor always has the potential to self start under steady wind conditions, whereas the starting of a two-bladed device is dependent upon its initial starting orientation.

Keywords: vertical axis wind turbines, Darrieus, wind turbine, self-starting

1 INTRODUCTION

The use of wind turbines for small-scale and urban applications is a topic that is receiving increasing attention. The relative merits of different turbine configurations, both vertical and horizontal axes, have been widely discussed and well summarized by many authors [**1**, **2**]. The work presented here is focused upon the Darrieus-type vertical axis machine. For small-scale applications, simplicity and low cost are of primary importance and in this regard, the Darrieus machine offers some distinct advantages relative to horizontal axis turbines, including accessible systems (often located at or close to the ground), low noise, and potentially simple blade design. Acknowledged disadvantages include the magnitude, location, and orientation of the peak blade stresses, the lack of an inherent blade speed limit which adds further complication to the stress problem, and lower efficiency than comparable axial machines although some would argue with the latter statement [**2**]. For domestic and small industrial applications, the issues of blade loading are relatively easily managed and efficiency, if it is indeed an issue, is of less importance than simplicity, cost, and reliability. Of potentially greater importance is the starting capability of these devices. Some researchers including Kentfield [**3**] have stated that the Darrieus turbine is inherently non self-starting whereas others have qualified this by stating that variable geometry or very careful aerofoil selection is required to promote self-starting [**1**, **2**]. For small-scale devices, a self-starting capability under typical wind conditions is essential and it is the investigation and numerical simulation of the physics of self-starting that is the focus of this study.

1.1 Self-starting

The term self-starting needs to be defined carefully. Ebert and Wood [**4**] define the starting process as having been completed when significant power extraction commences, and Kirke [**1**] deems a turbine to be self-starting only if it can accelerate from rest to the point where it starts to produce a

*Corresponding author: School of Engineering, University of Durham, South Road, Durham DH1 3LE, UK. e-mail: r.g.dominy@durham.ac.uk

useful output. In both cases, the definitions of the terms 'significant power' and 'useful output' are themselves imprecise. Others (e.g. Lunt [**5**]) have adopted a more specific definition by which a machine is deemed to have started if it has accelerated from rest to a condition where the blades operate at a steady speed that exceeds the wind speed (i.e. the tip speed ratio, $TSR > 1$). The basis of this definition is that to exceed a *TSR* of 1.0, the turbine can no longer be operating entirely as a drag device (a device in which the maximum blade speed cannot exceed the wind speed in the manner of a Savonius rotor) but that significant lift must be produced during the rotational cycle. Although more precise, this definition also has its limitations. In particular, there is evidence that reaching the point at which the blades begin to produce lift over a significant part of a revolution does not guarantee that the machine will to continue to accelerate. Baker [**6**] describes a dead band that may extend to *TSR*'s in excess of 2 in which there is insufficient or even negative torque that prevents further acceleration. He argues that when operating in this zone, only if the wind suddenly drops while the rotor inertia maintains its rotational speed can the tip speed ratio reach a value that is sufficient to drive the machine to a fully lifting state. The implication of this statement is that significant atmospheric wind transients are required to complete the self-starting process for a fixed-blade Darrieus turbine. The evidence that a Darrieus turbine using fixed geometry, symmetrical aerofoil blades cannot self-start would therefore seem compelling were it not for the many, but usually unsubstantiated, observations that devices of precisely this configuration do self-start in the field. In some of these cases, it may be that self-starting was induced by atmospheric gusting but that would not appear to be true in all cases. Whether a particular design self-starts will depend not only upon its aerodynamic performance but also upon the characteristics of any driven load and there seems to have been no systematic approach to the analysis of the aerodynamic characteristics of turbines in isolation from their resistive loads. Only when these factors are understood individually can the matching of a turbine and its load be performed effectively.

The purpose of this study is therefore to determine the fundamental physics associated with the starting process and to demonstrate conclusively whether, in principle, a simple Darrieus device is capable of self-starting. To achieve these objectives, a computational model has been developed to analyse the rotor performance from the moment it is released until a steady-state condition is achieved whether or not that condition provides useful torque. The model has been validated against published data and against observations from a small-scale wind tunnel model of a three-bladed Darrieus turbine.

1.2 Aerofoil performance characteristics

To understand the performance of the turbine, it is helpful to consider an individual aerofoil operating through one or more complete revolutions. The generic velocity vectors for an aerofoil operating at incidence are well known and apply to any moving aerofoil whether in isolation or as one of a set of blades in a turbine or cascade (Fig. 1). For most applications, an aerofoil is expected to operate in an unstalled condition and the relative incidence varies over only a few degrees even when operating off-design. However, for a vertical axis wind turbines (VAWT), the incidence initially changes through 360° during the single revolution of an individual blade and only when the blade speed exceeds the wind speed is this range reduced. The VAWT, therefore, experiences incidences that are more extreme than those experienced by almost any other aerofoil application under normal operating conditions.

To analyse the blade forces and hence the torque and power of the machine, it is necessary to know the lift and drag characteristics of its blades over the full incidence range. Such data are scarce; the most complete set arising from the work performed at the Sandia National Laboratories during the 1970s and 1980s, notably by Sheldahl and Klimas [**7**].

For the purpose of the analysis presented here, the symmetrical NACA 0012 aerofoil was chosen primarily because of its wide use for VAWT research. Most early Darrieus devices made use of NACA 0012 or 0015 sections although more recently some studies have indicated that performance advantage can be gained through the use of novel aerofoil shapes [**1**]. In the absence of explicit rules for the selection of aerofoils for Darrieus turbines, the NACA 0012 aerofoil was considered to be appropriate for this study. The complete lift and drag characteristics of this aerofoil are summarized in Fig. 2 for a range of

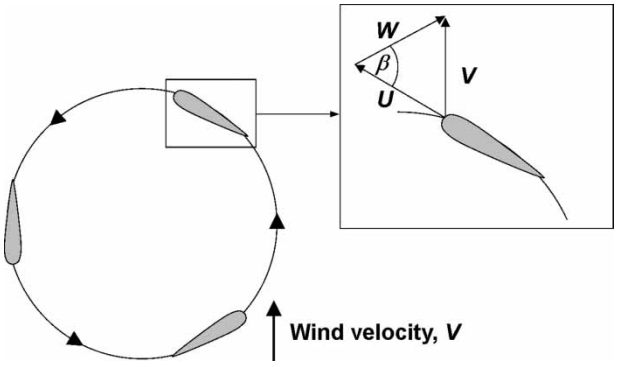

Fig. 1 Generic blade velocity triangle for a VAWT

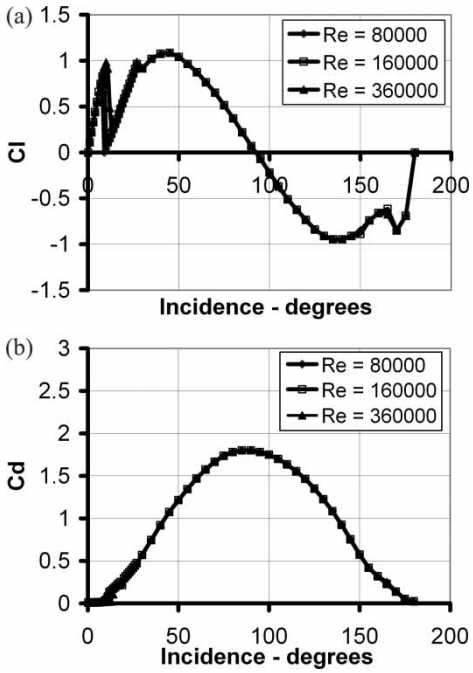

Fig. 2 NACA0012 lift and drag coefficients at three Reynolds numbers (data from reference [**7**])

Reynolds numbers that might be experienced during the operation of a 'small' VAWT in typical wind conditions ($<$10 m/s). For the purpose of this study, a small VAWT is defined as having a nominal power rating of $<$2.5 kW. In view of the shortage of data for this or any other aerofoil section in the stalled region, it is useful to make a comparison between the Sheldahl and Klimas [**7**] data and that of others in the more widely investigated unstalled and just post-stalled zone in order to gain confidence in that data (Fig. 3). However, such a comparison casts some doubt on the accuracy of the Sheldahl and Klimas [**7**] data in this region, and hence there must also be some uncertainty over the stalled zone data, but in the absence of a more reliable alternative most previous analysis has been based upon their unique data set. For this reason, new measurements were made at Durham University to investigate the aerodynamic performance of this and other aerofoils over the full incidence range. Only the NACA 0012 data are presented here and it is these data that have been used for the predictions of turbine startup performance (Fig. 4). The aerofoil had a chord of 0.15 m and a span of 0.45 m resulting in tested Reynolds numbers of up to 2×10^5. The blade tips extended to the side walls of the wind tunnel to eliminate tip leakage and hence the data approximate to a two-dimensional test case. The data of Sheldahl and Klimas suggest that Reynolds number effects are negligible in all but a small range of incidence close to and shortly after stall (Fig. 2). During start up, the blades operate at these critical incidences for only a very small time and hence as an acceptable approximation the startup performance has been analysed on the basis of the aerodynamic data derived from tests made at a single Reynolds number (1.7×10^5).

2 PERFORMANCE MODELLING

Modelling of the overall turbine performance was based on a time-stepping approach. For any initial, user-defined blade starting position, wind speed, and angular velocity, the resulting velocity triangle determines the relative airspeed and blade incidence for each blade. The lift and drag coefficients are found for this incidence by interpolation from a look-up table based on the blade aerodynamic database and hence the absolute forces are easily determined for the chosen aerofoil dimensions. For this study, no tip effects have been considered but the aspect ratio is high (span/chord = 13.3) so tip effects would not be expected to have a significant impact on the flow physics associated with startup.

Once the blade forces have been determined, the forces are resolved in the circumferential direction in order to establish the instantaneous torque and

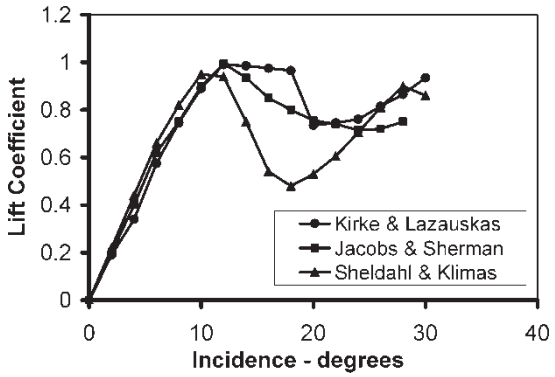

Fig. 3 Comparison of published NACA 0012 lift coefficient data

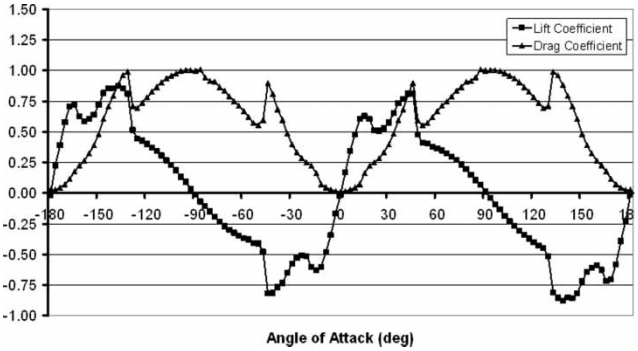

Fig. 4 Lift and drag coefficients for the NACA 0012 at $Re = 1.65 \times 10^5$

power. Knowing the inertial characteristics of the machine together with any resistance due to the bearing friction and generator load characteristics, the instantaneous acceleration of the rotor is calculated and applied over a short time interval to determine a new rotor position from which the process is repeated. The information from each time step is stored to allow a complete mapping of the time history of each variable included in the calculation. As long as the time increment is small in comparison to the changes of speed and acceleration, the time stepping approach provides an accurate model of the device. For multi-bladed machines, it is a simple task to sum the effects of each individual blade. For this work, a time increment of 0.001 s was used but such is the speed of even modest desktop PCs that much smaller periods can be used if required. A preliminary analysis of the results presented here confirmed that reducing the period by an order of magnitude had no significant effect and hence the larger interval was adopted to keep the size of the data set within acceptable bounds. In the absence of any directly relevant data, the impact of the wake generated by an upstream blade on its downstream neighbours was not considered during the course of this initial study.

3 RESULTS

Table 1 provides a summary of the geometric and numerical parameters used for this study. The turbine represents a potential domestic or light industrial unit rated at approximately 2.5 kW. The notation that is used for geometrical definitions and sign convention is shown in Fig. 5.

3.1 Single-bladed rotor

Initially, the starting characteristics of a single-bladed rotor are considered. Although this configuration is unlikely to be used for a practical machine, it provides a valuable tool to aid the visualization and explanation of the processes involved during startup.

Figure 6 shows the time history of the blade velocity based on a constant free stream wind speed of 10 m/s and an initial blade velocity of zero which represents the point at which any brake or locking

Table 1 Simulation parameters

Data for NACA 0012		Other physical constants	
Chord, c	0.15 m	Radius of rotation, R	1.20 m
Span, s	2.00 m	Air density, ρ	1.20 kg/m^{-3}
Mass, m	3 kg (each blade)	Wind speed, V	10 m/s

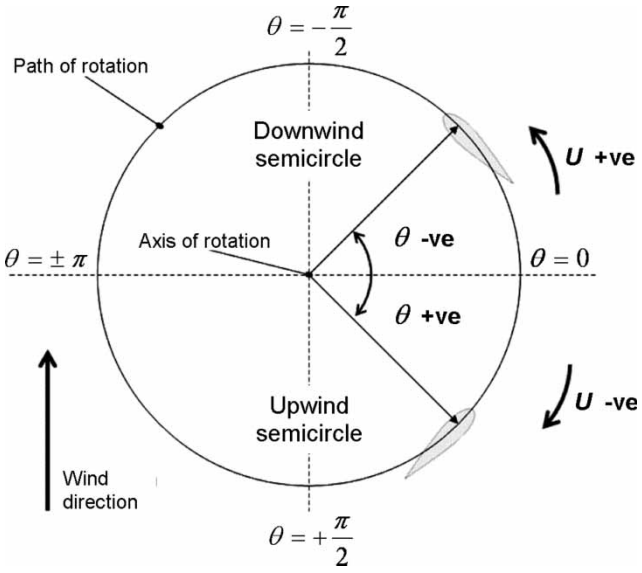

Fig. 5 Sign convention

mechanism is released. For this demonstration, the initial blade incidence was 45° at a starting position of $3\pi/4$.

In this instantaneous starting situation, although stalled, the circumferential component of lift is sufficient to accelerate the rotor forwards. Although the aerodynamic forces fluctuate as the rotor rotates and the blade incidence changes the rotor is able to maintain a continuous acceleration until it reaches a tip speed ratio of approximately 3.9.

Even at this apparently steady-state operation, there are very considerable torque variations around the cycle (Fig. 7(a)) which correspond to the blade incidence changes that occur (Fig. 7(b)) and to the corresponding variation of blade lift, drag, and net tangential force component (Fig. 7(c)). It should be noted that once a nominally steady-state condition has been achieved, the blade incidence never exceeds ± 0.25 rad (14.3°) and thus it remains unstalled. The choice of a 0.001 s time interval is not sufficiently small to capture exactly the true periodicity of the solution (most noticeable in Fig. 7(c)) but the observed error has little impact upon the essential characteristics and is only noticeable at the high tip speed ratios associated with a turbine in 'lift mode'.

The aerofoil data of Sheldahl (Fig. 2) and those presented here (Fig. 4) show that the lift characteristics of the aerofoil are qualitatively similar whether it is moving into the wind (0°–90°) or away from the wind (180°–90°). However, the drag is higher when reversed. Consequently, if the starting position is advanced through 90°, the tangential component of the drag is greater than the corresponding lift component and the blade therefore starts to move forwards, away from the wind (Fig. 8).

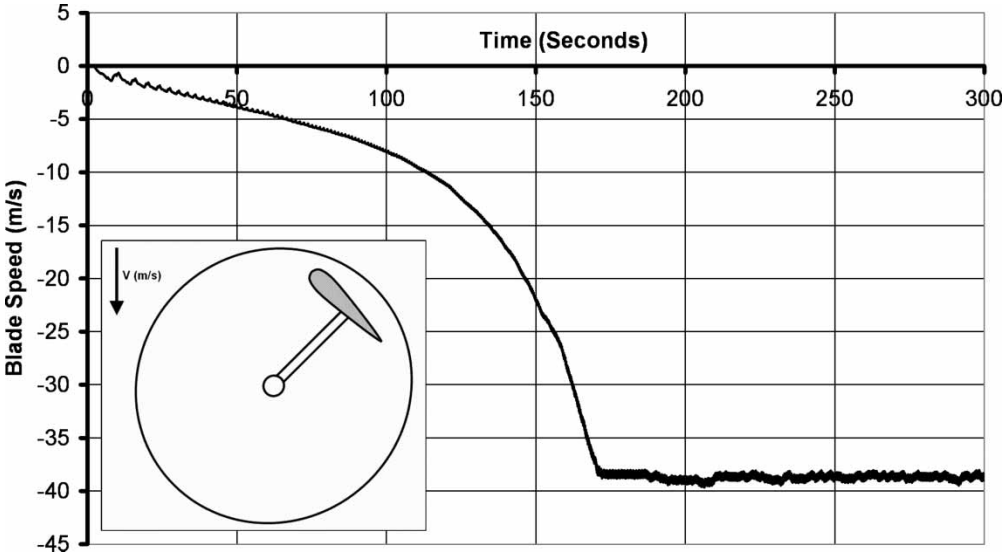

Fig. 6 Rotor acceleration from standstill (single blade; $+3\pi/4$ starting position)

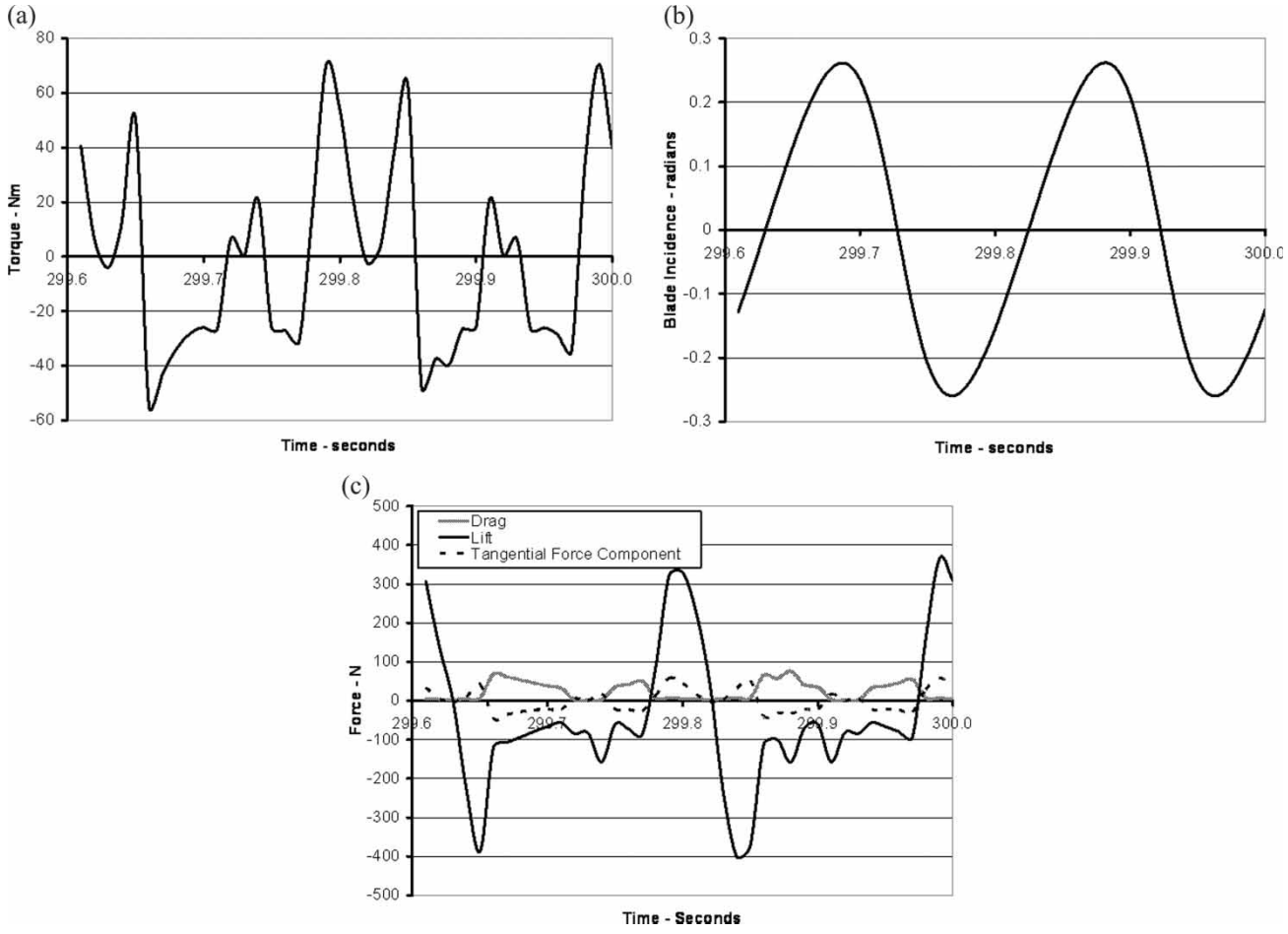

Fig. 7 Blade torque, incidence, and force changes during a single rotation: (a) rotor torque: single blade; $3\pi/4$ starting position, (b) blade incidence: single blade; $3\pi/4$ starting position, (c) blade forces: lift, drag, and net tangential component

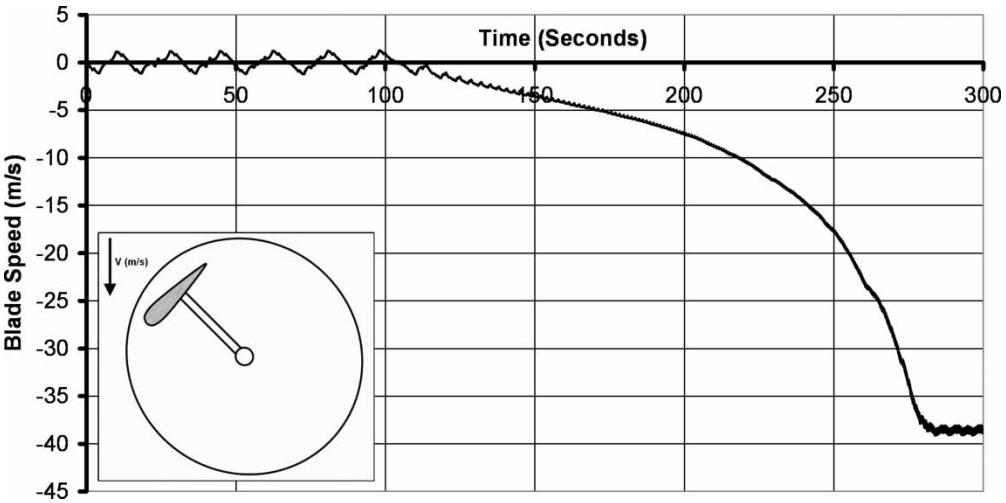

Fig. 8 Change of blade speed with time (single blade; $+\pi/4$ starting position)

As it progresses into the next quadrant, the tangential components of both the lift and the drag lift act in the same direction, thus further advancing the blade, but as the $-\pi/2$ position is approached those components approach zero, and as the blade passes into the third quadrant, both are reversed in direction thus beginning to slow the blade until at a position of approximately $-3\pi/2$ the blade motion is reversed. The blade does not return exactly to its initial starting position but moves through that position before stopping just a few degrees past it and reversing once again and repeating the cycle. However, the different starting position leads to a slightly exaggerated motion which grows each time it is repeated until after six cycles the motion is sufficient to carry the blade into the fourth quadrant. The significance of this is that the tangential component of the lift again acts in the forward direction, causing the blade to complete the revolution and allowing the turbine to accelerate quickly to its continuous operating condition, once again with a mean tip speed ratio of 3.9.

A third case of interest is where the blade lies initially across the wind at $-\pi/2$. If the forward and rearward halves of the aerofoil were symmetrical, there would be no net tangential force and the blade would remain in this stable position. For conventional aerofoil shapes, such as the NACA 0012, the asymmetry results in a small tangential force that moves the blade very slowly backwards. Any small change of position is sufficient to create a restoring force that moves the blade back, slightly past its initial position until the force is again reversed. This 'rocking' back and forth continues indefinitely and provides a low amplitude, periodic but essentially stable condition (Fig. 9).

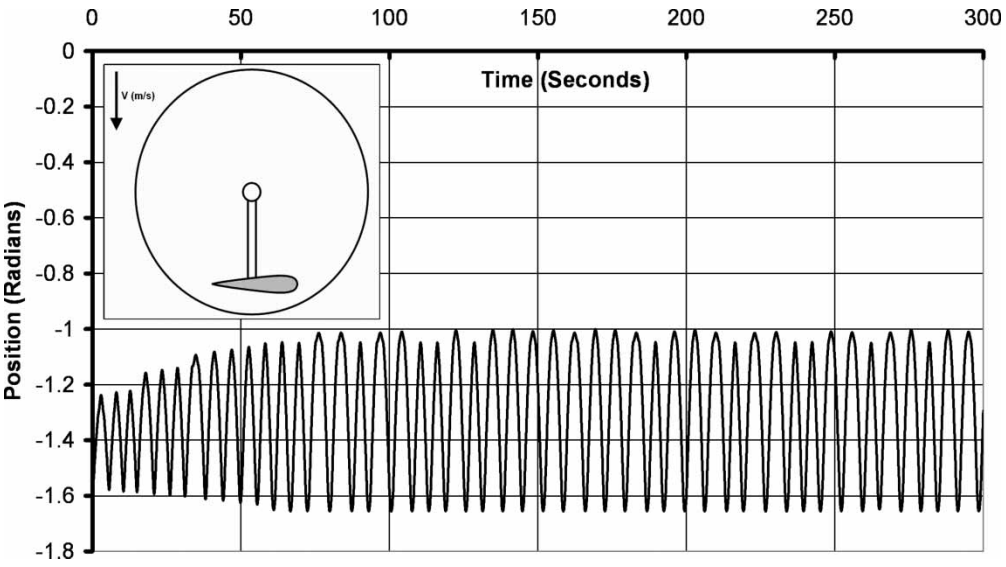

Fig. 9 Change of blade position with time (single blade; $-\pi/2$ starting position)

	Start Position, θ (radians)	Description of behaviour
a		Blade moves forwards across the wind and enters continuous rotation
b		Blade oscillates about its position, and then enters continuous rotation
c		Blade oscillates by ~ $3\pi/2$, starting forwards, with growing oscillations until continuous rotation is achieved
d		Blade oscillates about its position with growing oscillations. Oscillations suddenly grow to ~ $\pi/2$ in magnitude, then blade comes to rest at ~ $-\pi/2$.
e		Blade oscillates with growing oscillations and then comes to rest at ~ $-\pi/2$
f		Blade oscillates about its position ($\theta = -\pi/2$) and does not enter into continuous rotation. This is the '*neutral position*' of the blade.
g		Blade oscillates about $-\pi/2$
h		Blade oscillates about its position, suddenly begins oscillating by about $\pi/2$ backwards, then comes to rest at $-\pi/2$

Fig. 10 Single blade starting behaviour

It may be shown that any starting position will correspond to one of the three conditions described above or a combination of two of them. A complete summary of the rotor behaviour under all possible stationary starting positions is shown in Fig. 10.

3.2 Multi-bladed rotor

Using a similar approach it is easy to sum the effects of two or more blades to determine the characteristics of multi-bladed machines although if too many blades are adopted the solidity is likely to lead to blade wake interactions having a significant

	Start Position, θ (radians)	Description of behaviour
a	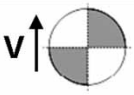	VAWT enters continuous rotation immediately
b		VAWT makes small oscillations then comes to rest. This is the '*neutral position*' of the machine.
c		VAWT makes small oscillations then enters continuous rotation
d	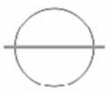	VAWT makes small oscillations, growing in size, then suddenly moves backwards by just more than $\pi/2$ and then enters continuous rotation

Fig. 11 Two-bladed rotor starting behaviour

	Start Position, θ (radians)	Description of behaviour
a		VAWT makes small oscillations then enters continuous rotation
b		VAWT makes small oscillations then enters continuous rotation
c		VAWT enters continuous rotation immediately
d		VAWT enters continuous rotation immediately

Fig. 12 Three-bladed rotor starting behaviour

influence on the turbine performance. Figure 11 provides a summary of the starting characteristics of a two-bladed rotor and Figure 12 provides equivalent data for a three-bladed device.

Simulations have been performed over a range of starting positions for one-, two-, and three-bladed rotors and the results are summarized in Fig. 13. This shows the startup time for each configuration against the starting position of the nominal 'primary' blade. A cut-off time of 300 s has been adopted on the basis that a machine that has not self-started by then is unlikely to do so and would certainly not be suitable for commercial operation.

It may be observed that the three-bladed rotor self-starts under all conditions at the datum wind speed of 10 m/s and that under a broad range of conditions its starting is almost instantaneous. The two-bladed rotor also self-starts under all conditions but there are four zones (approximately 0°, 90°, 180°, and 270°) where the capability to self-start is marginal including two (175°, 355°) that could be particularly problematic in a commercial device. Natural ambient turbulence may be sufficient to reduce these zones but, as yet, there is no experimental data to confirm this hypothesis. There are large zones in which the single-bladed rotor cannot self-start but this is not particularly surprising and it should be noted the starting times for this device have been included only to assist with the analysis of startup mechanisms and not as an analysis of a practical machine.

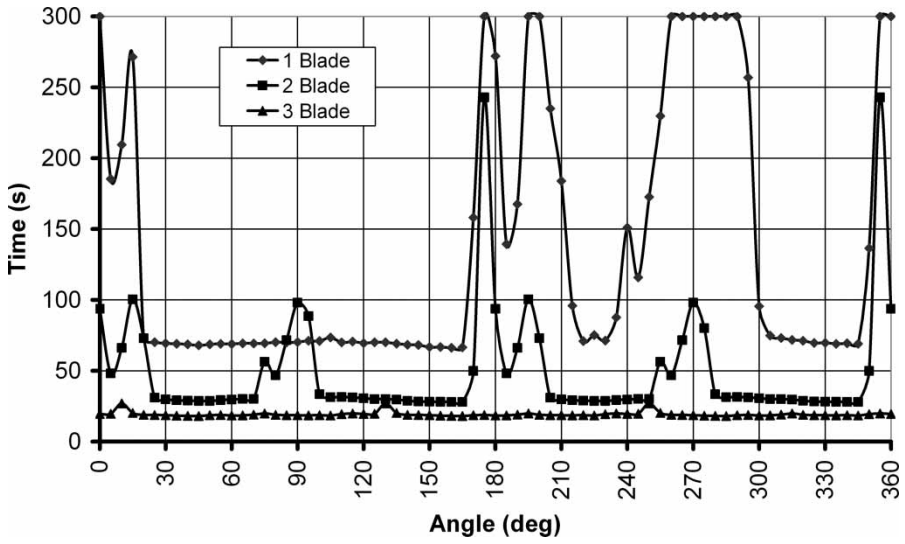

Fig. 13 Time to startup for a one-, two-, and three-bladed rotor from different starting positions

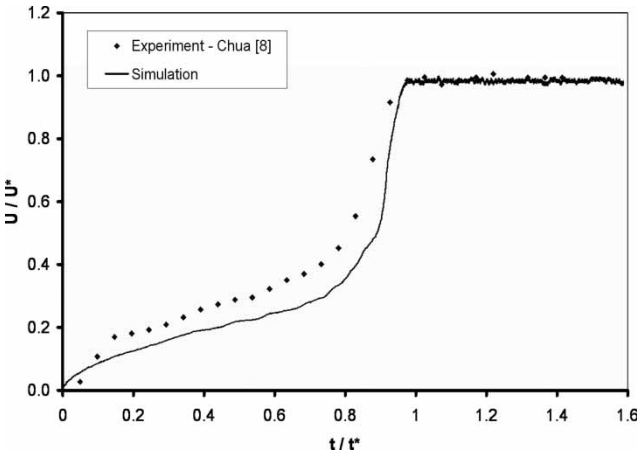

Fig. 14 Comparison between the normalized speed/time response of a real machine (unknown specification) [**8**] with simulation (specification approximated)

Very little rigorous experimental data are available to validate these predictions. The most useful is that of Chua [**8**] who provides a time history of rotor speed for a three-bladed machine. A detailed specification of the device was not provided by the author and the results can therefore only be used qualitatively but the comparison with normalized data generated using the model described here is highly encouraging (Fig. 14).

Further qualitative validation is provided by experiments that have been conducted on a smaller-scale but geometrically similar machine manufactured by Carbon Concepts Ltd. A sequence of photographs (Fig. 15) demonstrates the transition from a drag machine to a lift device during the starting process through the use of streamers attached to the upper blade tips. In Fig. 15(a), it is seen that blade 1 (left hand side of the photograph) is operating with a cross-flow component of approximately 90°. Blade 2 (foreground) also experiences a cross-flow but at reduced incidence and blade 3 (right hand side) is operating in its lifting zone and it is this blade that provides most of the drive. In Fig. 15(b), it is seen that the rotor has accelerated such that two of the three blades are operating in their unstalled, lifting mode with only blade 1 (left hand side) showing any sign of flow reversal. In Fig. 15(c), all three blades remain unstalled and in this mode the substantially higher tip speed ratio results in some blurring of the image but the streamers remain clearly visible.

All of the results that have been presented so far have been based on a nominal wind speed of 10 m/s. This is above the average UK wind speed and if small wind turbines are to be widely adopted it is essential that they are able to provide power at lower wind speeds. Figure 16 shows the predicted startup time required for a three-bladed rotor over a range of wind speeds based on a starting position of $\theta = \pi$ together with a line of best fit. It may be observed that as the ambient wind speed falls, the starting time increases but there is no discontinuity suggesting that ultimately the machine has the capacity to self-start over a very broad range of wind speeds. For all of the predictions presented here it has been assumed that the rotor has been only lightly loaded by the generator. This is not unreasonable since it is relatively simple to apply the electrical load only when a nominally steady state, lifting condition is reached. The introduction of the load would then influence the steady-state tip speed ratio and hence the power and torque generation but the fundamental aerodynamic starting process would be expected to remain unchanged.

4 CONCLUSIONS

The startup and continuous operation of various configurations of VAWT have been successfully modelled and validated based on the use of the NACA

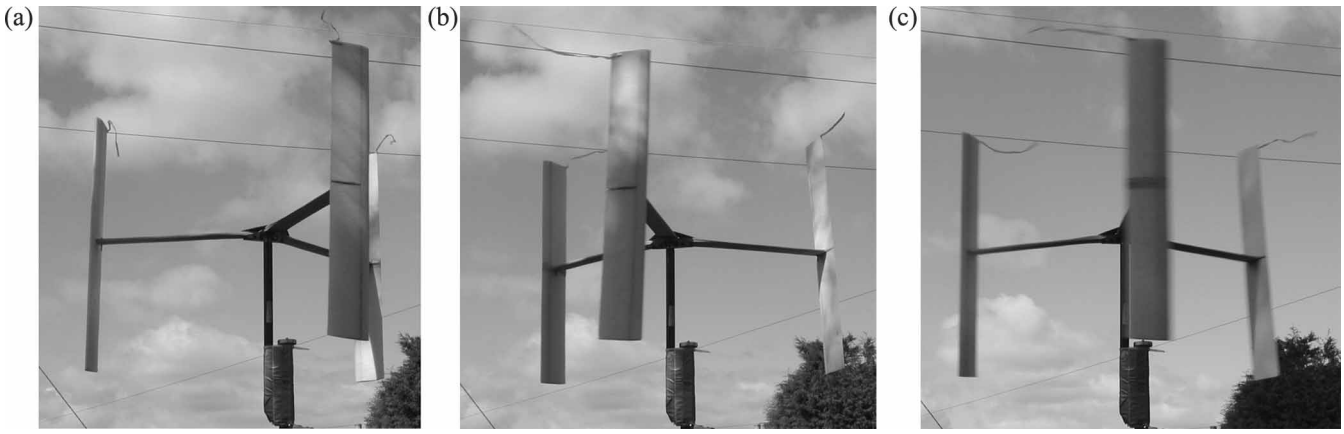

Fig. 15 VAWT staring behaviour from fully stalled to fully unstalled

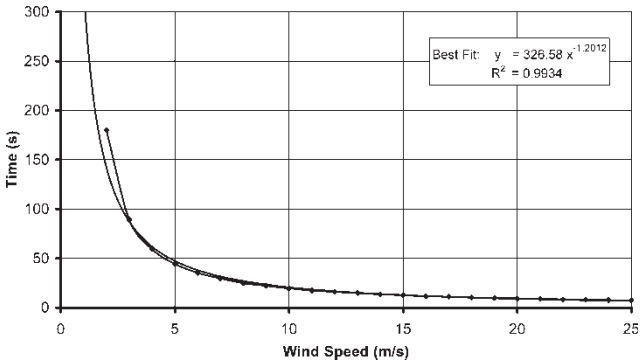

Fig. 16 Time to startup for a NACA 0012, three-bladed VAWT at different wind speeds

0012 aerofoil section operating at a nominal wind speed of 10 m/s. It has been shown that under lightly loaded conditions, two-bladed turbines have the potential to self-start but that the self-starting capability does not extend to all possible starting positions which could prove to be problematic for commercial turbines. However, it has been shown that a three-bladed rotor will self-start irrespective of its starting position. This has been confirmed by tests on a model turbine. It has also been shown that the three-bladed turbine is able to self-start at wind speeds that are much lower than the datum speed. It is therefore recommended that three-bladed designs should always be adopted in preference to two-bladed rotors if reliable self-starting is required.

REFERENCES

1 **Kirke, B. K.** *Evaluation of self-starting vertical axis wind turbines for stand-alone applications*. PhD Thesis, School of Engineering, Griffith University, Australia, 1998.
2 **Pawsey, N. C. K.** *Development and evaluation of passive variable-pitch vertical axis wind turbines*. PhD Thesis, School of Mechanical and Manufacturing Engineering, The University of New South Wales, Australia, 2002.
3 **Kentfield, J. A. C.** *The fundamentals of wind-driven water pumpers*, 1996 (Taylor and Francis, UK).
4 **Ebert, P. R.** and **Wood, D. H.** Observations of the starting behaviour of a small horizontal-axis wind turbine. *Renew. Energy*, 1997, **12**(3), 245–257.
5 **Lunt, P. A. V.** *An aerodynamic model for a vertical-axis wind turbine*. MEng project report, School of Engineering, University of Durham, UK, 2005.
6 **Baker, J. R.** Features to aid or enable self starting of fixed pitch low solidity vertical axis wind turbines. *J. Wind Eng. Ind. Aerodyn.*, 1983, **15**, 369–380.
7 **Sheldahl, R. E.** and **Klimas, P. C.** Aerodynamic characteristics of seven symmetrical aerofoil sections through 180-degree angle of attack for use in aerodynamic analysis of vertical axis wind turbines. SAND80-2114, Sandia National Laboratories, Albuquerque, USA, 1981.
8 **Chua, K. L.** Darrieus: Windturbine-analysis, 2002. Available from http://windturbine-analysis.com.

APPENDIX

Notation

c	blade chord (m)
m	blade mass (kg)
R	blade mean radius of rotation (m)
Re	reynolds number (dimensionless)
s	blade span (m)
t	time (s)
t^*	time taken to reach maximum blade (s)
TSR	tip speed ratio (U/V) (dimensionless)
U	blade speed (m/s)
U^*	maximum blade speed (m/s)
V	wind speed (m/s)
W	rotor relative wind speed (m/s)
β	blade relative flow angle (rad)
ρ	air density (kg/m^3)
ω	angular velocity (rad/s)